ACADEMIC PRESS

Available online at www.sciencedirect.com

SCIENCE DIRECT®

Journal of Sound and Vibration 260 (2003) 653–670

JOURNAL OF SOUND AND VIBRATION

www.elsevier.com/locate/jsvi

Free vibration of two identical circular plates coupled with bounded fluid

Kyeong-Hoon Jeong*

Mechanical System Development Department, Korea Atomic Energy Research Institute, P. O. Box 105, Yusong, Daejeon 305-600, South Korea

Received 1 August 2001; accepted 3 May 2002

Abstract

This paper examines the hydroelastic vibration of two identical circular plates coupled with a bounded fluid. An analytical method based on the finite Fourier–Bessel series expansion and the Rayleigh–Ritz method is suggested. In the theory, it is assumed that a rigid cylindrical container is filled with the ideal fluid and the two plates are clamped along the container edges. The proposed method is verified by finite element analysis using commercial software with excellent accuracy. Two transverse vibration modes, in-phase and out-of-phase, are observed alternately in the fluid-coupled system when the number of nodal circles increases for the fixed nodal diameter. It is found that the normalized natural frequency of the system monotonically increases with an increase in the number of nodal diameters and circles by virtue of a decrease in relative hydrodynamic mass.

1. Introduction

There have been many studies on the vibration of circular plates in contact with a fluid. The fluid-contacting structures have been used in mechanical engineering, such as in nuclear reactor internal components. Natural frequencies of the components have attracted extensive interest when exploring the structural responses to various excitations, such as seismic and pump pulsation excitations. The powerful numerical tools based on the finite element and boundary element methods make numerical solutions to fluid–structure interaction problems possible. However, the use of these methods requires enormous amounts of time for modelling and computation.

*Tel.: +82-42-868-8792; fax: +82-42-868-8990.
E-mail address: khjeong@kaeri.re.kr (K.-H. Jeong).

0022-460X/03/$ - see front matter
PII: S0022-460X(02)01012-X

Circular plates vibrating in contact with fluid have recently been studied. Kwak [1] and Kwak and Kim [2] studied the free vibrations of circular plates in contact with water on one side, while the free vibration of annular plates in contact with water on one side were investigated by Amabili et al. [3]. Kwak and Han [4] numerically and experimentally studied the effect of fluid depth on the natural frequency of a free edge circular plate. Amabili [5] also theoretically suggested a method to calculate the natural frequency of an annular plate in contact with a finite fluid domain on one side. They [1–5] considered the laterally unbounded fluid domain and also introduced the non-dimensionalized added virtual mass incremental (NAVMI) factors in order to estimate the fluid effect on the individual natural frequency of the fluid–structure coupled system. Chiba [6] obtained exact solutions for a circular elastic bottom plate in a cylindrical rigid tank filled with fluid. The elastic bottom plate supported by an elastic foundation and the free surface of the fluid was considered. Bauer [7] analytically determined the coupled natural frequencies of an ideal fluid in a circular cylindrical container of which a flexible membrane or elastic plate covered the free surface of the fluid. De Santo [8] carried out an experimental investigation of perforated circular plates submerged in water. Montero de Espinosa and Gallego-Juárez et al. [9] studied the vibration of plates submerged in water giving attention mainly to the lower modes using an approximate analytical method and experiments. Hagedorn [10] dealt with the theoretical free vibrations of an infinite elastic plate in water. Robinson and Palmer [11] performed a modal analysis of a flat rectangular plate floating on a body of liquid. They derived the transfer function for a harmonic point load, but the analysis is valid only for a finite number of lower frequency modes. However, these problems [1–11] are of a fundamentally different nature. Jeong et al. [12] theoretically treated the dynamics of two identical circular disks coupled with bounded fluid using Rayleigh's quotient in conjunction with an assumed-mode method. However, they could not predict the natural frequencies of the out-of-phase modes well.

This paper studies the coupling effects of contacting fluid on the free vibration characteristics of two identical circular plates with clamped edges. It is assumed that the contained fluid is incompressible, irrotational and frictionless and radially bounded by a rigid wall. The dynamic displacements of the plates are expanded in terms of the eigenfunctions of the plates in a vacuum with unknown weighting coefficients and then the Rayleigh–Ritz method is applied. The coefficients are determined by the boundary conditions along the edges of the plates and the compatibility requirement on the surface of the plates in contact with the fluid. Finally, the frequency equation for the coupled natural frequencies can be derived. The in-phase and out-of-phase natural frequencies of the fluid-coupled system can be obtained by theoretical calculations and verified by finite element analyses. The natural frequency of the wet mode is normalized with respect to the natural frequency of the dry mode in order to estimate the relative hydrodynamic mass effect on each coupled vibration mode of the circular plates.

2. Theoretical background

2.1. Formulation for circular plates

Fig. 1 shows two identical circular plates coupled with fluid, where R and $h(\ll R)$ represent the radius and thickness of the circular plates, respectively. The fluid domain is surrounded

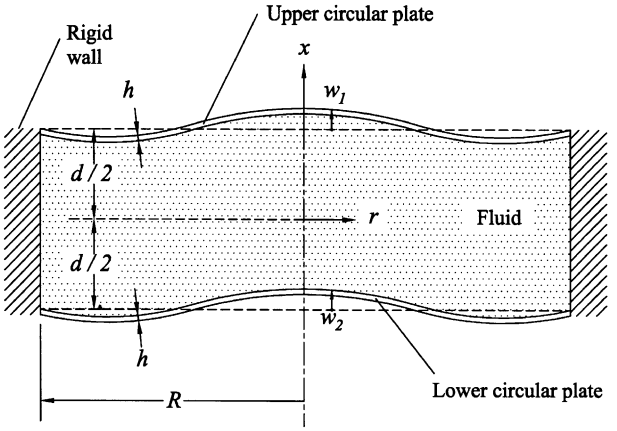

Fig. 1. Two identical circular plates coupled with bounded fluid.

by the two circular plates and the rigid cylindrical container. The following assumptions are made for the theoretical formulation: (a) the fluid motion is small; (b) the fluid is incompressible, inviscid and irrotational; (c) the circular plates are made of linearly elastic, homogeneous, and isotropic material; and (d) the shear deformation and rotary inertia are negligible. The equation of motion for the transverse displacement, w_j, of these circular plates is

$$D\nabla^4 w_j + \rho h w_{j,tt} = P_j, \quad j = 1, 2, \tag{1}$$

where $D = Eh^3/12(1-\mu^2)$ is the flexural rigidity of the circular plates; ρ, μ, E and P_j are the density, the Poisson ratio, Young's modulus of the plates and the hydrodynamic pressure on the circular plates, respectively. The comma in the equation denotes a partial derivative with respect to the corresponding variable and t is the time. The upper circular plate is referred to with subscript "1" while the lower one is denoted by subscript "2." In addition, ∇^4 in Eq. (1) represents the bi-harmonic operator in the polar co-ordinates r and θ. In order to find the mode shapes of the two plates in contact with a fluid, the Rayleigh–Ritz method is applied. Therefore, each wet mode shape can be expanded in a series by using a finite number of admissible function W_{nmj}, $m = 0, 1, 2, \ldots, M$, and appropriate unknown coefficients q_m and p_m. The choice of the admissible function is very important to simplify the calcuations and to guarantee convergence to the actual solution. For an arbitrary nodal diameter n ($n = 0, 1, 2, \ldots$) of the circular plates, the wet mode shapes w_1 and w_2 can be assumed in the form of

$$\begin{aligned} w_1(r,\theta,t) &= w_1(r,\theta)\exp(\mathrm{i}\omega t) \\ &= \cos(n\theta)\sum_{m=1}^{M} q_m W_{nm}(r)\exp(\mathrm{i}\omega t) \quad \text{for the upper plate,} \end{aligned} \tag{2a}$$

$$w_2(r,\theta,t) = w_2(r,\theta)\exp(\mathrm{i}\omega t)$$

$$= \cos(n\theta)\sum_{m=1}^{M} p_m W_{nm}(r)\exp(\mathrm{i}\omega t) \quad \text{for the lower plate,} \tag{2b}$$

$$\mathrm{i} = \sqrt{-1}, \tag{2c}$$

where ω is the fluid-coupled natural frequency of the plates. The admissible function, $W_{nm}(r)$ and $W_{nm}(r)$, can be assumed to be the eigenfunctions of the plates in a vacuum which satisfy the boundary conditions along the plate edges. So, m represents the number of nodal circles of the plates in a vacuum, or the number of expanding terms for the radial modal function. When we consider the geometric boundary conditions along the edge of the plates, the displacement must be zero for the clamped boundary condition, that is, $W_{nm} = W_{nm} = 0$ at $r = R$. Therefore, the modal displacements of Eq. (2) will be reduced to

$$W_{nm}(r) = J_n(\lambda_{nm}r) - J_n(\lambda_{nm}R)I_n(\lambda_{nm}r)/I_n(\lambda_{nm}R). \tag{3}$$

The frequency parameter for the plates, λ_{nm}, can be obtained using the boundary condition for the zero slope, i.e., $\mathrm{d}W_{nm}/\mathrm{d}r = 0$ at $r = R$:

$$J_n(\lambda_{nm}R)I_{n+1}(\lambda_{nm}R) + J_{n+1}(\lambda_{nm}R)I_n(\lambda_{nm}R) = 0. \tag{4}$$

The trial function, W_{nm}, is linearly independent, orthogonal and constitute a complete set. J_n and I_n of Eqs. (3) and (4) are the Bessel function and the modified Bessel function of the first kind, respectively.

2.2. Velocity potential

We consider the fluid region by which two identical circular plates and the rigid cylindrical wall are surrounded. The facing side of the circular plates is in contact with an ideal fluid. It is also assumed that the fluid is bounded in the radial direction at $r = R$. The three-dimensional oscillatory fluid flow in the cylindrical co-ordinates can be described with the velocity potential. The fluid movement induced by vibration of the plates is described with the general velocity potential that satisfies the Laplace equation:

$$\nabla^2\Phi(r,\theta,x,t) = 0. \tag{5}$$

It is possible to separate the function Φ with respect to r, θ, and x. Thus,

$$\Phi(r,\theta,x,t) = \mathrm{i}\omega\phi(r,\theta,x)\exp(\mathrm{i}\omega t), \tag{6}$$

where ϕ is the spatial velocity potential. The general solution of Eq. (5) for the arbitrary nodal diameter n can be obtained using the separation of variables:

$$\phi(r,\theta,x) = \sum_{s=1}^{\infty} J_n(\beta_{ns}r)\{E_{ns}\sinh(\beta_{ns}x) + F_{ns}\cosh(\beta_{ns}x)\}\cos(n\theta), \tag{7}$$

where the coefficients β_{ns} can be determined by the following transcendental equation with respect to every s and n:

$$J_n'(\beta_{ns}R) = 0, \tag{8}$$

where Eq. (8) satisfies the boundary condition along the rigid wall surface and this means zero radial velocity at $r = R$:

$$\frac{\partial\phi(r,\theta,x)}{\partial r} = 0 \quad \text{at } r = R. \tag{9}$$

When we consider the symmetry of the fluid velocities for the in-phase and out-of-phase vibration modes, the velocity potential will require the following symmetric conditions:

$$\frac{\partial\phi(r,\theta,-x)}{\partial x} = \frac{\partial\phi(r,\theta,x)}{\partial x} \quad \text{for the in-phase modes,} \tag{10a}$$

$$\frac{\partial\phi(r,\theta,x)}{\partial x} = 0 \quad \text{at } x = 0 \quad \text{for the out-of-phase modes.} \tag{10b}$$

Application of Eqs. (10a) and (10b) gives simple reduced forms of Eq. (7) for the in-phase and out-of-phase modes:

$$\phi(r,\theta,x) = \sum_{s=1}^{\infty} E_{ns} J_n(\beta_{ns} r)\sinh(\beta_{ns} x)\cos(n\theta) \quad \text{for the in-phase modes,} \tag{11a}$$

$$\phi(r,\theta,x) = \sum_{s=1}^{\infty} F_{ns} J_n(\beta_{ns} r)\cosh(\beta_{ns} x)\cos(n\theta) \text{for the out-of-phase modes.} \tag{11b}$$

2.3. Method of solution

In Eqs. (2a) and (2b), the symmetry of the modal displacements will give the relationship between the coefficients q_m and p_m:

$$q_m = p_m \quad \text{for the in-phase modes,} \tag{12a}$$

$$q_m = -p_m \quad \text{for the out-of-phase modes.} \tag{12b}$$

In order to determine the unknown coefficients E_{ns} and F_{ns} of fluid motion in Eqs. (11a) and (11b), the compatibility conditions at the interface of the upper and lower plates in contact with the fluid are used. Compatibility conditions at the fluid interface with the plates yield

$$w_1(r,\theta) = -\frac{\partial\phi}{\partial x} \quad \text{at } x = d/2, \tag{13a}$$

$$w_2(r,\theta) = -\frac{\partial\phi}{\partial x} \quad \text{at } x = -d/2. \tag{13b}$$

Substitution of Eqs. (2a), (2b), (3), (11a), (11b), (12a) and (12b) into Eqs. (13a) and (13b) gives

$$\sum_{m=1}^{M} q_m[J_n(\lambda_{nm} r) - J_n(\lambda_{nm} R) I_n(\lambda_{nm} r)/I_n(\lambda_{nm} R)]$$
$$= -\sum_{s=1}^{\infty} E_{ns}\beta_{ns}\cosh\left(\frac{\beta_{ns} d}{2}\right) J_n(\beta_{ns} r) \quad \text{for the in-phase modes,} \tag{14a}$$

$$\sum_{m=1}^{M} q_m \left[J_n(\lambda_{nm} r) - J_n(\lambda_{nm} R) I_n(\lambda_{nm} r) / I_n(\lambda_{nm} R) \right]$$

$$= -\sum_{s=1}^{\infty} F_{ns} \beta_{ns} \sinh\left(\frac{\beta_{ns} d}{2}\right) J_n(\beta_{ns} r) \quad \text{for the out-of-phase modes.} \tag{14b}$$

Expanding $J_n(\lambda_{nm} r)$ and $I_n(\lambda_{nm} r)$ of Eqs. (14a) and (14b) into the Bessel–Fourier series [13] gives

$$J_n(\lambda_{nm} r) = \sum_{s=1}^{\infty} a_{nms} J_n(\beta_{ns} r), \tag{15a}$$

$$I_n(\lambda_{nm} r) = \sum_{s=1}^{\infty} b_{nms} J_n(\beta_{ns} r), \tag{15b}$$

where

$$a_{oms} = \frac{-2(\lambda_{om} R) J_1(\lambda_{om} R)}{[(\beta_{os} R)^2 - (\lambda_{om} R)^2] J_o(\beta_{os} R)} \quad \text{for } n = 0, \tag{16a}$$

$$b_{oms} = \frac{2(\lambda_{om} R) I_1(\lambda_{om} R)}{[(\beta_{os} R)^2 + (\lambda_{om} R)^2] J_o(\beta_{os} R)} \quad \text{for } n = 0, \tag{16b}$$

$$a_{nms} = \frac{2(\beta_{ns} R)^2 (\lambda_{nm} R) J_n'(\lambda_{nm} R)}{[(\beta_{ns} R)^2 - n^2]\,[(\beta_{ns} R)^2 - (\lambda_{nm} R)^2] J_n(\beta_{ns} R)} \quad \text{for } n = 0, \tag{16c}$$

$$b_{nms} = \frac{2(\beta_{ns} R)^2 (\lambda_{nm} R) I_n'(\lambda_{nm} R)}{[(\beta_{ns} R)^2 - n^2][(\beta_{ns} R)^2 + (\lambda_{nm} R)^2] J_n(\beta_{ns} R)} \quad \text{for } n > 0. \tag{16d}$$

Therefore, the velocity potential of the fluid can be written in terms of unknown constant q_m instead of unknown coefficients E_{ns} or F_{ns} by arrangement of Eqs. (12a), (12b), and (14a)–(16d)

$$\phi(r, \theta, x) = \sum_{m=1}^{M} q_m \sum_{s=1}^{\infty} \Xi_{nms} J_n(\beta_{ns} r) \sinh(\beta_{ns} x) \cos(n\theta) \quad \text{for the in-phase modes,} \tag{17a}$$

$$\phi(r, \theta, x) = \sum_{m=1}^{M} q_m \sum_{s=1}^{\infty} \Xi_{nms} J_n(\beta_{ns} r) \cosh(\beta_{ns} x) \cos(n\theta) \quad \text{for the out-of-phase modes,} \tag{17b}$$

where Ξ_{nms} is a derived coefficient:

$$\Xi_{nms} = -\frac{\left[a_{nms} - b_{nms} J_n(\lambda_{nm} R)/I_n(\lambda_{nm} R)\right]}{\beta_{ns} \cosh(\beta_{ns} d/2)} \quad \text{for the in-phase modes,} \tag{18a}$$

$$\Xi_{nms} = -\frac{\left[a_{nms} - b_{nms} J_n(\lambda_{nm} R)/I_n(\lambda_{nm} R)\right]}{\beta_{ns} \sinh(\beta_{ns} d/2)} \quad \text{for the out-of-phase modes.} \tag{18b}$$

In order to perform numerical calculations for each fixed n value, a sufficiently large finite M number of terms must be considered in all the previous sums of the expanding term, m. For this

purpose, a vector $\mathbf{q}$ of the unknown parameters is introduced as depicted in Refs. [3,5]:

$$\mathbf{q} = \{ q_1 \quad q_2 \quad q_3 \ldots \quad q_M \}^{\mathrm{T}}. \tag{19}$$

Now it is necessary to know the reference kinetic energies of the plates and the containing fluid in order to calculate the coupled natural frequencies of the circular plates in contact with fluid. Using the hypothesis of irrotational movement of the fluid, the reference kinetic energy of the fluid can be evaluated from its boundary motion:

$$\begin{aligned} T_F^* = & \tfrac{1}{2}\rho_o \int_0^{2\pi} \int_0^R (\partial\phi(r,x)/\partial x)_{x=d/2} \phi(r,d/2) \cos^2(n\theta) r \, \mathrm{d}r \, \mathrm{d}\theta \\ & - \tfrac{1}{2}\rho_o \int_0^{2\pi} \int_0^R (\partial\phi(r,x)/\partial x)_{x=-d/2} \phi(r,-d/2) \cos^2(n\theta) \, r \, \mathrm{d}r \, \mathrm{d}\theta, \end{aligned} \tag{20}$$

where ρ_o is the mass density of fluid. Application of Eqs. (13a) and (13b) into Eq. (20) reduces to:

$$T_F^* = -\tfrac{1}{2}\rho_o \kappa_\theta \left(\int_0^R w_1 \phi(r,d/2) r \, \mathrm{d}r + \int_0^R w_2 \phi(r,-d/2) r \, \mathrm{d}r \right), \tag{21}$$

where $\kappa_\theta = 2\pi$ for $n = 0$ and $\kappa_\theta = \pi$ for $n > 0$. Insertion of Eqs. (2), (3) and (17a), (17b) into Eq. (21) gives the reference kinetic energy of the fluid:

$$T_F = \rho_o \kappa_\theta \mathbf{q}^{\mathrm{T}} \mathbf{G} \mathbf{q}, \tag{22}$$

where the $M \times M$ symmetric added virtual mass incremental (AVMI) matrix [2] $\mathbf{G}$ for the fixed n is given by Eqs. (15a)–(16d) and (18a), (18b).

$$G_{ik} = \sum_{s=1}^{\infty} \frac{8(\beta_{ns}R) R^3 \Lambda_{is} \Lambda_{ks} H_{ns}}{[(\beta_{ns}R)^2 - n^2]}, \quad i,k = 1,2,\ldots,M, \tag{23}$$

with

$$\Lambda_{is} = \frac{(\lambda_{ni}R)^3 J_n'(\lambda_{ni}R)}{[(\beta_{ns}R)^4 - (\lambda_{ni}R)^4]}, \tag{24a}$$

$$\Lambda_{ks} = \frac{(\lambda_{nk}R)^3 J_n'(\lambda_{nk}R)}{[(\beta_{ns}R)^4 - (\lambda_{nk}R)^4]}, \tag{24b}$$

$$H_{ns} = \tanh(\beta_{ns}d/2) \quad \text{for the in-phase modes,} \tag{25a}$$

$$H_{ns} = \coth(\beta_{ns}d/2) \quad \text{for the out-of-phase modes.} \tag{25b}$$

When $n = 0$ and $s = 1$, the first term of G_{ik} has a zero denominator and a zero numerator at the same time for the in-phase modes because $\beta_{ns} = 0$. The limit of the first term of G_{ik} must be determined as β_{ns} approaches zero. In consequence of formulation, the first term of G_{ik} for the in-phase modes with $n = 0$ will be replaced with $4dR^2 J_1(\lambda_{0i}R) J_1(\lambda_{0k}R)/[(\lambda_{0i}R)(\lambda_{0k}R)]$ instead of the

first term of Eq. (23). On the other hand, when $n = 0$ and $s = 1$, the first term of G_{ik} for the out-of-phase modes must be replaced with $8R^4J_1(\lambda_{0k}R)J_0(\lambda_{0i}R)/[(\lambda_{0i}R)^2(\lambda_{0k}R)d]$ instead of the first term of Eq. (23). In Eq. (23), the sum on s must be stopped for numerical computation, at an integer value large enough to give the required accuracy.

The reference kinetic energy of the two circular plates, as obtained by using the orthogonality of mode shapes, is given by

$$T_d = \rho h \kappa_\theta \mathbf{q}^{\mathrm{T}} \mathbf{Z} \mathbf{q}, \tag{26}$$

where $\mathbf{Z}$ is the $M \times M$ matrix defined by

$$Z_{ik} = \delta_{ik} \int_0^R r W_{ni} W_{nk} \, \mathrm{d}r, \quad \delta_{ik} : \text{Kronecker delta}. \tag{27}$$

When Eq. (3) is inserted into Eq. (27) and the integration is carried out, one obtains a simple expression:

$$Z_{ik} = R^2 \{J_n(\lambda_{ni}R)\}^2 \delta_{ik}. \tag{28}$$

The maximum potential energy of the two plates can be computed as a sum of the kinetic energies of the dry eigenfunctions,

$$V_d = \kappa_\theta D \int_0^R \left([\nabla^2 w_1]^2 - 2(1-\mu) \left\{ (w_{1,rr}) \left(\frac{w_{1,r}}{r} + \frac{w_{1,\theta\theta}}{r^2} \right) - \left(\left[\frac{w_{1,\theta}}{r} \right], r \right)^2 \right\} \right) r \, \mathrm{d}r. \tag{29}$$

As the first term $[\nabla^2 w_1]^2$ in Eq. (29) is identical to $\lambda_{ni}^4 w_1^2$ and the other terms of Eq. (29) are negligible compared with the first term, the maximum potential energy is given by

$$V_d \approx \kappa_\theta D \mathbf{q}^{\mathrm{T}} \mathbf{P} \mathbf{q}, \tag{30}$$

where $\mathbf{P}$ is the $M \times M$ diagonal matrix defined by

$$P_{ik} = (\lambda_{ni}R)^4 \{J_n(\lambda_{ni}R)\}^2 \delta_{ik}/R^2. \tag{31}$$

In Eq. (30), the correspondence between the reference total kinetic energy of each mode multiplied by its square circular frequency and the maximum potential energy of the same mode is used. In order to find the coupled natural frequencies and wet mode shapes of the two plates in contact with fluid, the Rayleigh quotient for the plates vibration coupled with an ideal fluid is used:

$$V_d/(T_d + T_F). \tag{32}$$

Minimizing the Rayleigh quotient with respect to unknown parameters q_m, the non-dimensional Galerkin equation can be obtained:

$$D\mathbf{P}\mathbf{q} - \omega^2(\rho h \mathbf{Z} + \rho_o \mathbf{G})\mathbf{q} = \{0\}. \tag{33}$$

Eq. (33) gives an eigenvalue problem and the coupled natural frequency ω can be calculated.

3. Examples and discussion

3.1. Theoretical and finite element models

On the basis of the preceding analysis, in order to find the natural frequencies of two identical circular plates coupled with radially bounded fluid by the cylindrical rigid wall, the determinant of the left side in Eq. (33) is calculated using the commercial software Mathcad [14]. The frequency equation derived in the preceding sections involves double series expansions of algebraic terms. In the theoretical calculation, the Bessel–Fourier expansion term s is set at 200 and the expanding term m for the admissible function is set at 40, and setting so gives a converged solution.

Additionally, in order to check the validity of the theory, the finite element analysis is also carried out for the bounded fluid-coupled system using the commercial computer code, ANSYS (release 5.6). The finite element model is constructed with the same plate geometry, boundary conditions and material properties used in the theoretical calculation. The plates are made of aluminum having a radius of 120 mm and a thickness of 2 mm. The distance between the circular plates, d, is 40 mm. The physical properties of the material are as follows: Young's modulus = 69.0 GPa, the Poisson ratio = 0.3, and mass density = 2700 kg/m^3. Water, having a density of 1000 kg/m^3, is used as the fluid in contact with the plates. The viscosity of water is neglected in the theoretical calculation and the finite element analysis.

Finite element analysis using ANSYS software [15], is performed to obtain the natural frequencies of the two identical plates coupled with bounded fluid. For the finite element method (FEM) analysis, a two-dimensional model is constructed with axisymmetric harmonic fluid elements (FLUID81) and axisymmetric harmonic shell elements (SHELL61). The fluid element 'FLUID81' with four nodes has three degrees of freedom at each node and it is particularly well suited for calculating hydrostatic pressures and fluid–structure interactions. The shell element 'SHELL61' with two nodes has four degrees of freedom. The fluid domain is divided into a number of identical fluid elements and the upper and lower plates are also divided into shell elements. The nodes of the fluid elements at $r = 0$ are constrained in the radial direction only. On the other hand, the fluid movement at $r = R$, namely along the rigid cylindrical wall, is restricted to the radial direction only. The vertical velocity of the fluid element nodes adjacent to each surface of the wetted circular plates coincides with those of circular plates so that the finite element model can simulate Eqs. (13a) and (13b). Each circular plate is divided into 24 two-dimensional axisymmetric shell elements of the same size and the fluid region of the finite element model consists of 192 (8×24) fluid elements as illustrated in Fig. 2. A clamped boundary condition along each plate edge is applied in the finite element model. A sufficient number of master degrees of freedom is selected to calculate 30 modal frequencies between 100 and 8000 Hz. In the finite element modal analysis, some fluid motion modes appear when the lower frequency limit to be considered is less than that of the fluid motion modes because the bulk modulus of the elasticity of water is considered. Only fluid motion without structural vibration is observed at the fluid motion modes. The fluid motion modes are similar to the sloshing modes of fluid with a free surface and the frequency of these modes is usually lower than that of fluid-coupled structural vibration modes. Therefore, the lower frequency limit is set at 100 Hz in order to avoid extracting the fluid motion modes. In the finite element analysis, the reduced method is used for the

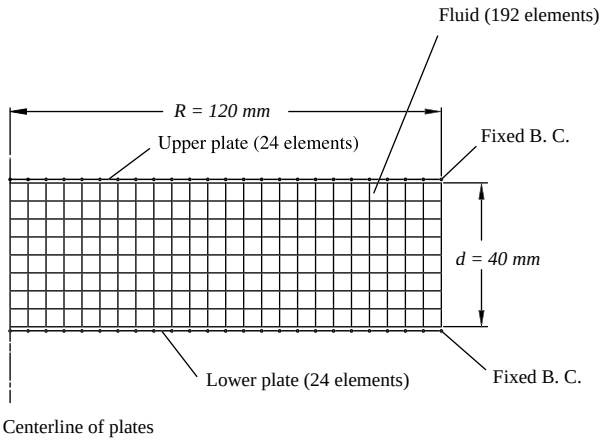

Fig. 2. Finite element model for two identical circular plates coupled with fluid.

eigenvalue and eigenvector extractions, which employs the Householder-Bisection-Inverse iteration extraction technique.

3.2. Theoretical and finite element results

All of the mode shapes can be classified into two transverse vibration mode categories according to the relative moving directions between the two plates during the vibration; that is, in-phase and out-of-phase modes, appear as shown in Fig. 3. The coupled natural frequency of the plates with $d = 40$ mm for out-of-phase and in-phase modes are listed in Table 1. The symbol m' in Figs. 4 and 5 and Table 1 represents the number of nodal circles in a vibration mode. In the range of $0 \leqslant n \leqslant 4$ and $0 \leqslant m' \leqslant 3$, it is found that the theoretical natural frequencies agree well with the finite element results within 1% error range for the in-phase mode. For the out-of-phase mode, the maximum deviation of the theoretical natural frequency from the finite element result is about 5.6% when the mode is $n = 0$, $m' = 1$. However, the deviations for the out-of-phase modes are also less than 1% except the case of mode ($n = 0$, $m' = 1$) as shown in Table 1.

The coupled natural frequency of the two plates in contact with fluid is always less than the corresponding natural frequency of the plate in a vacuum, due to contribution of the hydrodynamic mass to the motion of the plates. Hence, the normalized natural frequencies, defined as the natural frequency of a structure in contact with a fluid divided by the corresponding natural frequency of the structure in a vacuum, always lie between unity and zero.

Especially, the out-of-phase mode with $n = 0$ and $m' = 0$ cannot appear because the mode violates the fluid volume conservation. The second fluid-coupled natural frequency ($n = 0, m' = 1$) of the out-of-phase mode is reduced to 31.1% of the natural frequency of the plate in a vacuum. On the other hand, for the corresponding in-phase mode of the same case, it is reduced to 50.4% of the natural frequency of the dry mode. The in-phase mode of the plates is mostly generated by the fluid movement in the vertical direction. On the other hand, the out-of-phase modes of the plates are created with the combined-fluid movement in the vertical and radial directions as shown in the vector plots of Fig. 4. As an increase of the number of nodal diameters (n) or nodal circles (m') cannot effectively restrict the vertical movement of the fluid, the normalized natural

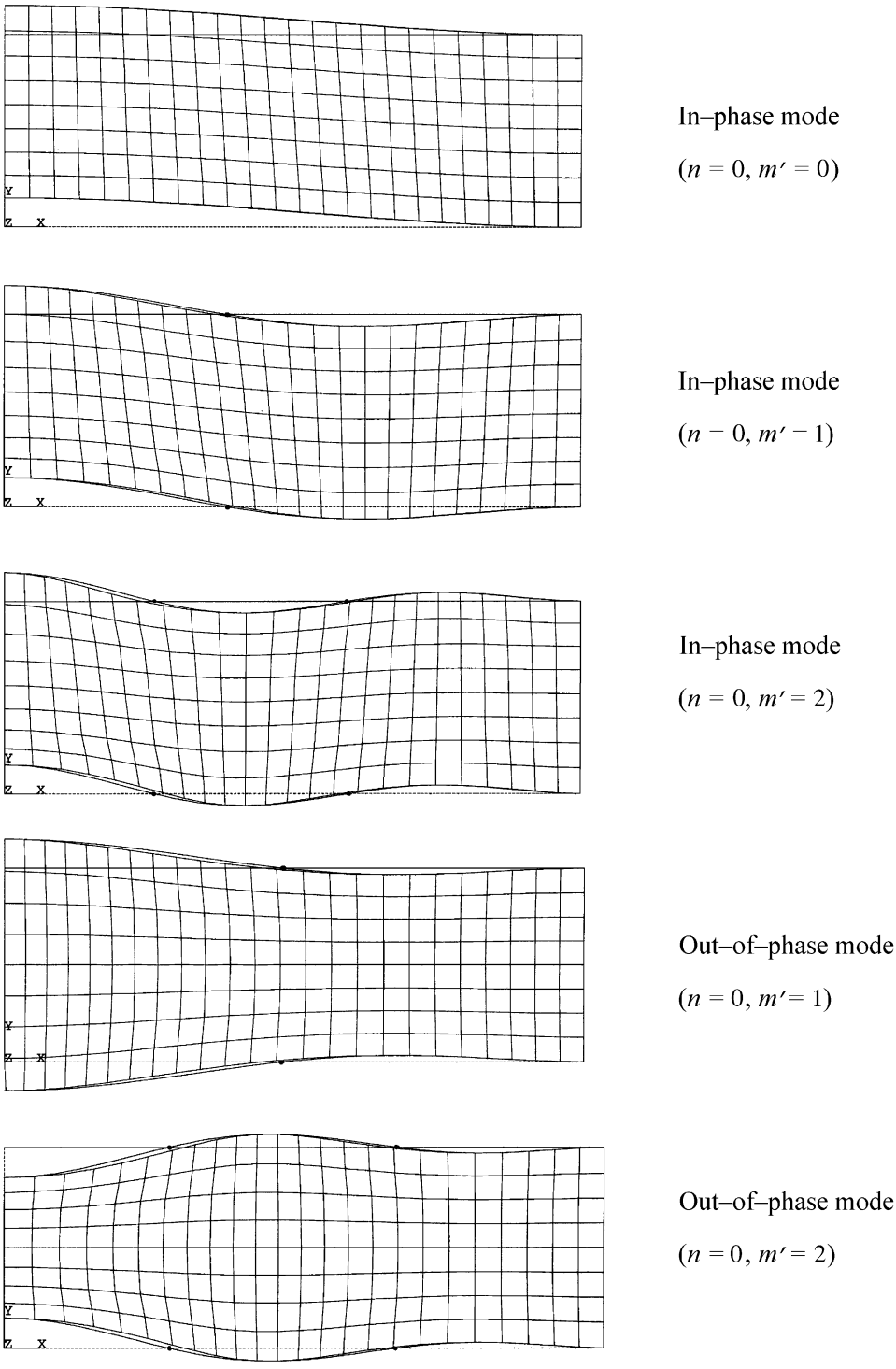

Fig. 3. Mode shapes of two circular plates coupled with fluid.

Table 1
Comparison of FEM and theoretical natural frequencies (Hz) for two identical circular plates coupled with bounded fluid

Mode		Coupled natural frequency (Hz)								
		In vacuum			Fluid-coupled case					
					In-phase mode			Out-of-phase mode		
n	m'	FEM	Theory	Discrepancy (%)	FEM	Theory	Discrepancy (%)	FEM	Theory	Discrepancy (%)
0	0	345.4	345.5	0.03	162.7	162.8	0.06	N/A	N/A	N/A
	1	1344.4	1344.9	0.04	676.9	677.5	0.09	399.7	377.4	−5.58
	2	3010.4	3013.1	0.09	1645.0	1642.8	−0.13	1339.3	1347.7	0.63
	3	5340.4	5349.1	0.16	3156.9	3141.2	−0.50	2869.4	2883.8	0.50
1	0	718.8	718.9	0.01	348.3	348.4	0.03	147.3	147.5	0.14
	1	2055.7	2057.0	0.06	1077.5	1076.3	−0.11	786.7	785.6	−0.14
	2	4055.5	4060.6	0.13	2308.4	2298.4	−0.43	2018.9	2011.8	−0.04
	3	6717.2	6731.1	0.21	4120.1	4083.6	−0.89	3850.9	3830.4	−0.53
2	0	1179.0	1179.4	0.03	589.0	589.5	0.08	365.8	366.1	0.08
	1	2857.7	2860.2	0.09	1553.6	1552.4	−0.08	1282.5	1281.5	−0.08
	2	5193.0	5201.4	0.16	3059.0	3046.1	−0.42	2802.4	2795.1	−0.26
	3	8186.9	8207.8	0.25	5171.3	5126.4	−0.87	4929.1	4907.8	−0.43
3	0	1724.7	1725.6	0.05	889.5	890.9	0.16	667.0	667.8	0.12
	1	3749.9	3754.3	0.12	2109.7	2109.0	−0.03	1872.5	1872.5	0.00
	2	6422.4	6435.3	0.20	3901.5	3886.9	−0.34	3683.5	3677.1	−0.17
	3	9749.2	9778.8	0.30	6319.9	6268.5	−0.81	6108.8	6087.6	−0.34
4	0	2354.1	2355.8	0.07	1253.4	1256.2	0.22	1046.2	1048.1	0.18
	1	4730.9	4737.9	0.15	2747.5	2748.3	0.03	2548.0	2549.9	0.07
	2	7742.5	7761.3	0.24	4836.0	4820.7	−0.03	4656.0	4651.0	−0.11
	3	—	11443.6	—	7565.5	7509.0	−0.75	7385.7	7363.7	−0.30

Table 1
Comparison of FEM and theoretical natural frequencies (Hz) for two identical circular plates coupled with bounded

frequency of in-phase modes gradually increases according to the increase of the number of nodal diameters or nodal circles. On the contrary, the normalized natural frequency of the out-of-phase modes drastically increases with an increase in the number of nodal diameters and nodal circles by virtue of the separation of the fluid flow direction. That is to say, for the out-of-phase mode of $n = 0$ and $m' = 1$ shown in Fig. 4(c), the lateral fluid flow to the center of the plate is divided into two parts and the stroke of the fluid movement is shortened when the number of nodal circles increases to 2, as shown in Fig. 4(d). The second out-of-phase mode has a less amount of fluid flow. An increase of the number of nodal circles or nodal diameters reduces an added mass and eventually it contributes to the increase of the normalized natural frequencies. Therefore, the separation effect of the fluid flow direction is dominant in the case of out-of-phase modes because an increase of the number of nodal circles effectively restricts the fluid movement in the radial direction. When the number of the nodal diameters or the nodal circles increases, the

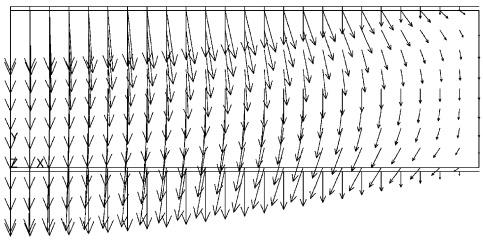

(a) In–phase mode of $n = 0$, $m' = 0$

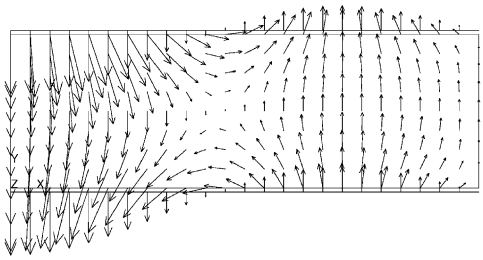

(b) In–phase mode of $n = 0$, $m' = 1$

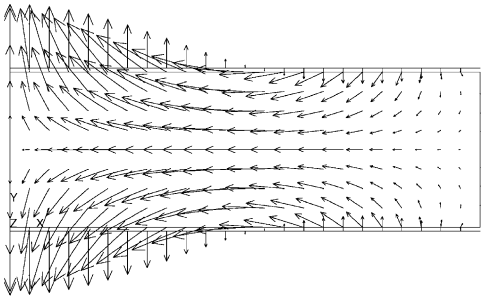

(c) Out–of–phase mode of $n = 0$, $m' = 1$

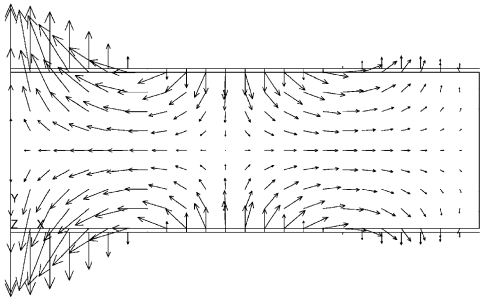

(d) Out–of–phase mode of $n = 0$, $m' = 2$

Fig. 4. Displacement vector plot for the in-phase and out-of-phase mode mode shapes.

corresponding natural frequencies converge together as illustrated in Fig. 5, because the global fluid movement changes to local fluid movement and eventually the hydrodynamic mass effect on the systematic kinetic energy reduces.

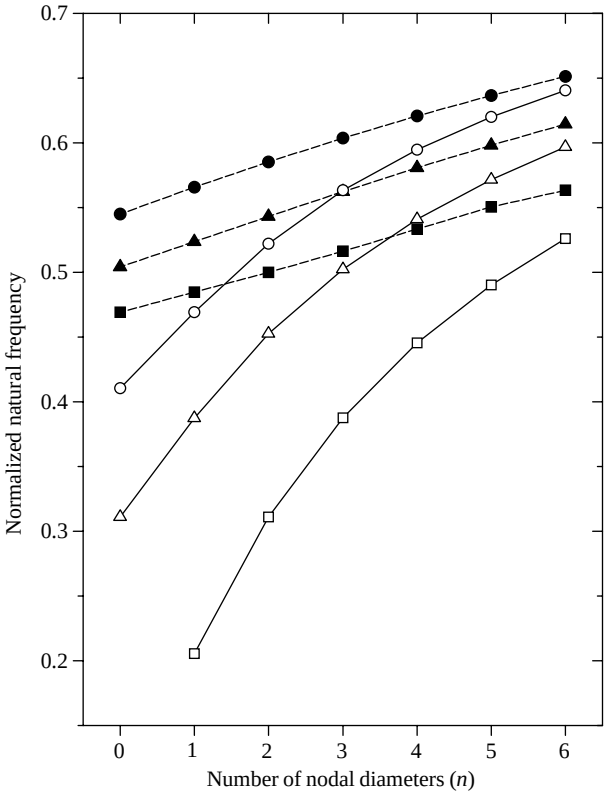

Fig. 5. Normalized natural frequencies of the fluid-coupled two circular plates: - - - - -, in-phase mode; ——, out-of-phase mode; – –■– –, $m' = 0$; – –▲– –, $m' = 1$; – –●– –, $m' = 2$; —□—, $m' = 0$; —△— $m' = 1$; —○—, $m' = 2$.

Generally speaking, the wet mode shapes are different from the corresponding dry mode shapes except in some special cases. When we focus on the structural mode shapes in contact with fluid, the deviation from the dry mode shapes depends not only on the coupling area between the structure and the fluid, but also on the amount of moving fluid. Figs. 6 and 7 obtained by the finite element analyses illustrate a comparison between the dry and wet mode shapes of the circular plate. There is little difference between the normalized in-phase mode shapes and the corresponding dry mode shapes because the in-phase modes are free from the fluid volume conservation requirement. However, for the out-of-phase mode, the fluid volume conservation requirement makes a deviation from the dry mode shape. The mode shapes of Fig. 7(a) illustrate the out-of-phase and dry mode shapes for $n = 0$, $m' = 1$. The nodal circle of the dry mode appears at $r = 0.379R$ but it comes out at $r = 0.464R$ for the out-of-phase mode. If the nodal circle of the out-of-phase mode appears at the same nodal circle position of the dry mode, the remaining fluid of the fluid region must disappear or the extra fluid must be added. It violates the fluid volume conservation. Hence, the fundamental nodal circle move from $r = 0.379R$ to $0.464R$, when the circular plates in contact with fluid vibrate with the mode of $n = 0$ and $m' = 1$. The other out-of-phase modes are also built by not only the equilibrium among the plate stiffness, the plate mass

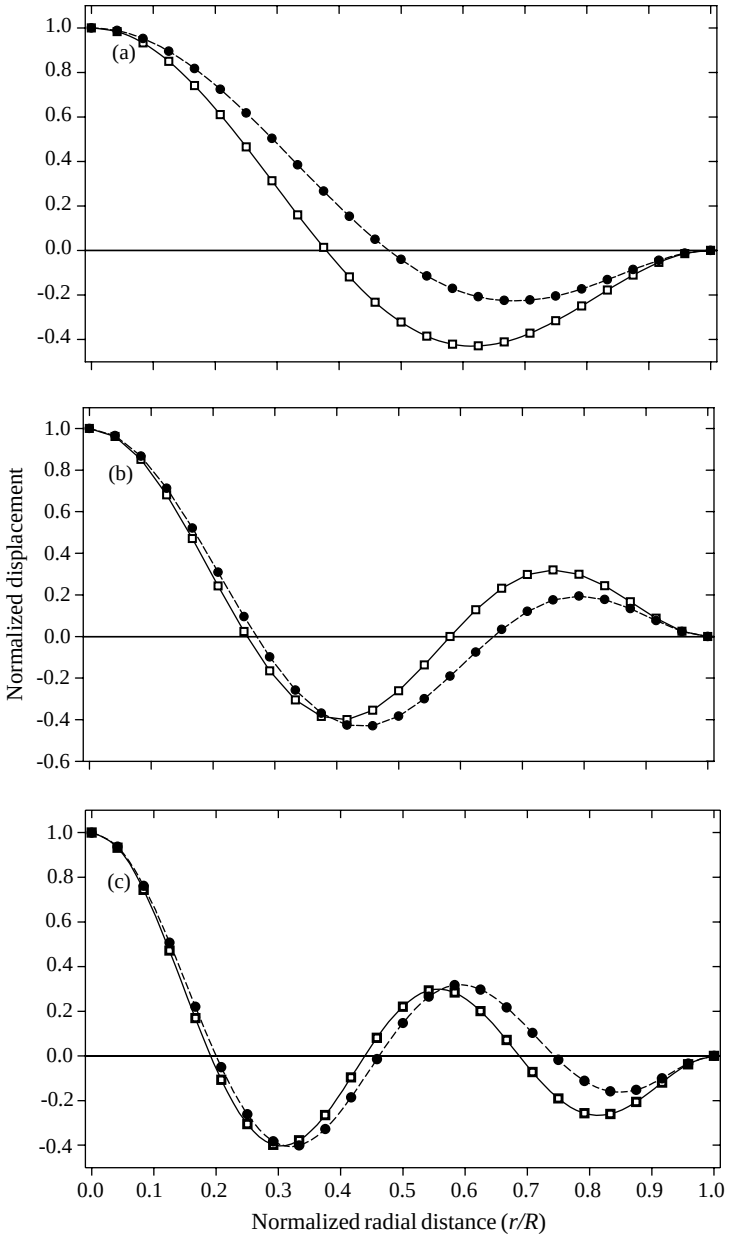

Fig. 6. Comparison of mode shapes for $n = 0$: —□—, dry and in-phase mode; - -●- -, out-of-phase mode. (a) $m' = 1$, (b) $m' = 2$, and (c) $m' = 3$.

and the fluid mass but also the requirement of the fluid volume conservation. Additionally, it is found that the difference between wet mode shapes according to the fluid gap size is negligible.

Fig. 8 demonstrates the fluid gap size effect on the normalized natural frequencies for the out-of-phase and in-phase modes. When the distance between the plates or the fluid gap, changes from

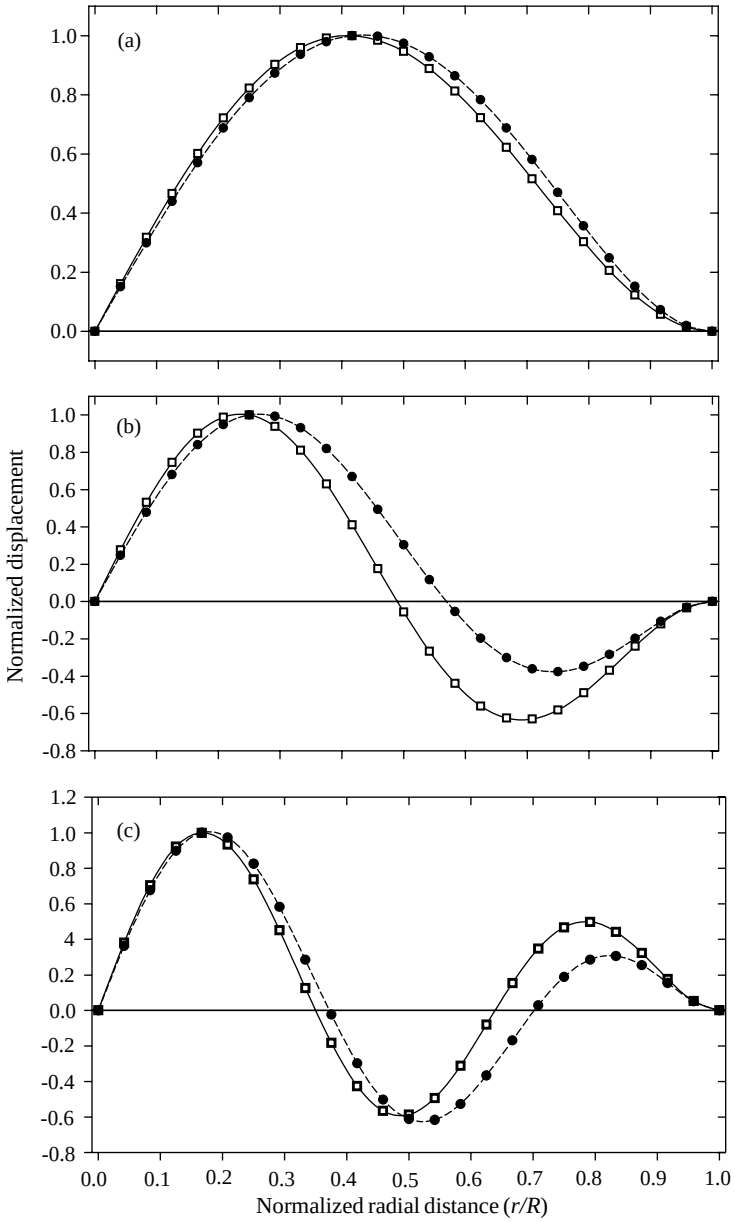

Fig. 7. Comparison of mode shapes for $n = 1$: —□—, dry and in-phase mode: - -●- -, out-of-phase mode. (a) $m' = 1$, (b) $m' = 2$, and (c) $m' = 3$.

$d = 20$ to 40 mm, the normalized natural frequency for the second out-of-phase mode ($n = 1$ and $m' = 1$) increases from 0.370 to 0.446. On the contrary, for the corresponding in-phase mode, the increase of the fluid gap reduces the normalized natural frequency from 0.613 to 0.531. It is found that the normalized natural frequency for the out-of-phase mode increases with an increase of the fluid gap regardless of mode numbers, but it is opposite to that for the in-phase mode. Eventually,

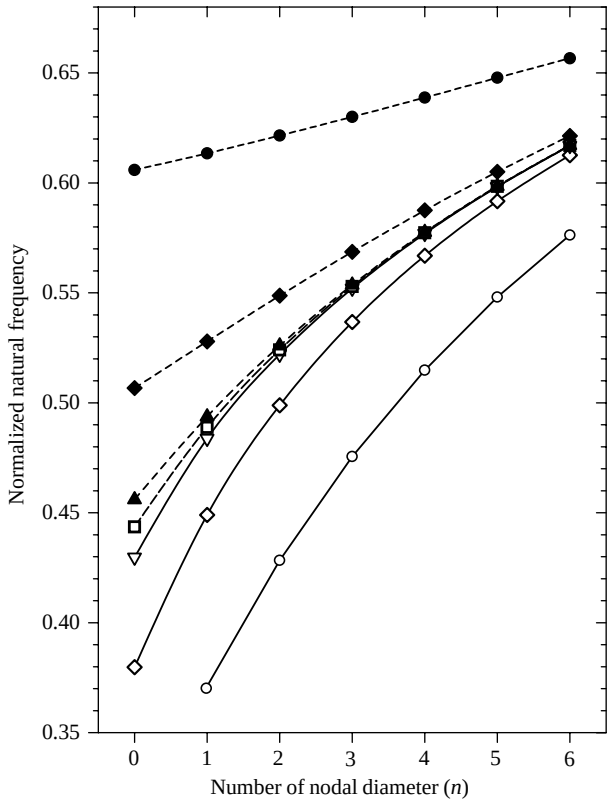

Fig. 8. Fluid gap effect on the normalized natural frequency for $m' = 1$: —○—, $d = 20$ mm; out-of-phase; —◇—, $d = 40$ mm, out-of-phase; —▽—, $d = 80$ mm, out-of-phase; --□--, $d =$ infinite; --●--, $d = 20$ mm, in-phase; --◆--, $d = 40$ mm, in-phase; --▲--, $d = 80$ mm, in-phase.

each normalized natural frequency of the two contrastive modes converges to the result of an infinite fluid gap. It is also observed that a reduction in the fluid gap significantly affects the coupled natural frequencies when $d < R$. The reduction of the fluid gap tends to enlarge the hydraulic coupling effect for the out-of-phase modes and reduces the natural frequency. However, for the same situation, the natural frequency of the in-phase mode increases by reduction of the amount of fluid mass itself and not by the coupling effect.

4. Conclusions

An analytical method to estimate the natural frequencies of two identical circular plates coupled with an ideal fluid is developed by the Rayleigh–Ritz method and the finite Fourier–Bessel series expansion method. It is observed that the two contrastive modes, the so-called out-of-phase and in-phase modes, appear alternately in the fluid-coupled system. It is verified that the theoretical approach can predict the coupled natural frequencies well. Especially, the theory based on the Rayleigh–Ritz method can predict the natural frequency of the in-phase mode precisely. It

is found that the normalized natural frequencies monotonically increase when the number of diametrical or circular modes increases owing to the division of the fluid flow during vibration.

Acknowledgements

This work has been carried out under the Nuclear R&D Program by the MOST of Korea.

References

[1] M.K. Kwak, Vibration of circular plates in contact with water, Transactions of the American Society of Mechanical Engineers, Journal of Applied Mechanics 58 (1991) 480–483.
[2] M.K. Kwak, K.C. Kim, Axisymmetric vibration of circular plates in contact with fluid, Journal of Sound and Vibration 146 (1991) 381–389.
[3] M. Amabili, G. Frosali, M.K. Kwak, Free vibrations of annular plates coupled with fluids, Journal of Sound and Vibration 91 (1996) 825–846.
[4] M.K. Kwak, S.B. Han, Effect of fluid depth on the hydroelastic vibration of free-edge circular plate, Journal of Sound and Vibration 230 (2000) 171–185.
[5] M. Amabili, Effect of finite fluid depth on the hydroelastic vibrations of circular and annular plates, Journal of Sound and Vibration 193 (1996) 909–925.
[6] M. Chiba, Axisymmetric free hydroelastic vibration of a flexural bottom plate in a cylindrical tank supported on an elastic foundation, Journal of Sound and Vibration 169 (1994) 387–394.
[7] H.F. Bauer, Coupled frequencies of a liquid in a circular cylindrical container with elastic liquid surface cover, Journal of Sound and Vibration 180 (1995) 689–704.
[8] D.F. De Santo, Added mass and hydrodynamic damping of perforated plates vibrating in water, Transactions of the American Society of Mechanical Engineers, Journal of Pressure Vessel Technology 103 (1981) 175–182.
[9] F. Montero de Espinosa, J.A. Gallego-Juárez, On the resonance frequencies of water-loaded circular plate, Journal of Sound and Vibration 94 (1984) 217–222.
[10] P. Hagedorn, A note on the vibrations of infinite elastic plates in contact with water, Journal of Sound and Vibration 175 (1994) 233–240.
[11] N.J. Robinson, S.C. Palmer, A modal analysis of a rectangular plate floating on an incompressible liquid, Journal of Sound and Vibration 142 (1990) 435–460.
[12] K.H. Jeong, T.W. Kim, S. Choi, K.B. Park, Free vibration analysis of two circular disks coupled with fluid, Proceedings, Technologies in Reactor Safety, Fluid–Structure Interaction, Sloshing and Natural Hazards Engineering, PVP-Vol. 366, pp. 157–164, 1998.
[13] I.N. Sneddon, Fourier Transforms, McGraw-Hill, New York, 1951.
[14] Mathcad User's Guide-Mathcad 2000 Professional, MathSoft, Inc, Cambridge, MA, 1999.
[15] P. Kohnke, ANSYS Theory Reference, ANSYS Elements Reference, ANSYS Command Reference, Release 5.4, SAS IP, Inc., Canonsburg, PA, 1997.